

# Glazing of tool dies for semi-solid steel forming

D. Brabazon<sup>1</sup>, S. Naher<sup>2</sup>, P. Biggs<sup>3</sup>

<sup>1</sup>Materials Processing Research Centre

URL: <http://www.mecheng.dcu.ie/MPRC/Introduction.htm>

e-mail: [dermot.brabazon@dcu.ie](mailto:dermot.brabazon@dcu.ie)

<sup>2</sup>Materials Processing Research Centre

URL: <http://www.mecheng.dcu.ie/MPRC/Introduction.htm>

e-mail: [sumsun.naher@dcu.ie](mailto:sumsun.naher@dcu.ie)

<sup>3</sup>Materials Processing Research Centre

URL: <http://www.mecheng.dcu.ie/MPRC/Introduction.htm>

e-mail: [patrick.biggs2@mail.dcu.ie](mailto:patrick.biggs2@mail.dcu.ie)

**ABSTRACT:** This paper describes an analysis conducted into the effect of CO<sub>2</sub> laser processing parameters on the surface modification and heat treatment of steels. The CO<sub>2</sub> laser and in house developed apparatus for movement of the samples allowed for high speed surface heat treatment. The operation of these components in conjunction allowed a wide variation in the heat treatments and sample properties to be obtained. In particular, the mechanism to pass the steel samples at high speeds (700 – 1200 mm/s), kept the focus spot exposure times below  $1 \times 10^{-3}$  s. Laser power from 825 to 1050W and continuous beam mode were used. Both laser hardened and laser glazed samples were analysed using optical microscopy, Vickers and micro hardness testing, and XRD. The samples showed functionally graded surface morphologies and corresponding hardness and stiffness responses. For more rapidly process samples three layers of distinct hardness were noted. In all cases crystal and property modification to approximately 500 $\mu$ m was found. Results show how the laser treatment is directly related to the hardness profile through the surface and resultant microstructures. The results from all the samples show increased hardness due to (a) the formation of martensite and ferrite in the laser hardened samples and (b) a complete microstructural transformation to an amorphous state in the glazed samples. It is noted that the higher stiffness and hardness of the glazed samples can expect to result in a more wear resistant coating for the semi-steel forming process. The amorphous layer may also be expected to act as a thermal barrier to the higher temperatures encountered in semi-solid steel forming.

Key words: Glazing, H13, laser processing, amorphous, XRD

## 1 INTRODUCTION

For a steel of eutectoid composition, in order to obtain a structure which is entirely martensitic the steel must be cooled quickly. This rate must be such that when plotted on a Time Temperature Transition plot for the alloy it does not cut into the ‘nose’ of the modified ‘transformation’ curve, in the region of 550°C. If the steel remains in this temperature range for even more than one second, then transformation to pearlite begins. Severe water-quenches are therefore required to produce wholly martensitic structures in the plain carbon steels [1].

For steel containing less than 0.3% carbon, it is impossible to obtain a wholly martensitic structure

however rapidly it is cooled. Large quantities of ferrite will inevitably precipitate when the transformation curve is unavoidably cut in the upper temperature ranges.

Fortunately, the addition of small amount of alloying elements such as chromium, nickel and manganese has the effect of slowing down transformation rates so that the TTT curves are displaced to the right of TTT plot. This means that much slower rates of cooling can be used, in the form of oil- or even air-quenches in order to obtain a martensitic structure.

H13 (wt%: 5.5Cr, 1.8Mo, 1.2V, 1.2Si, 0.5Mn, 0.45C, 0.3Ni, bal. Fe) steel is one of the most popular hot-working die steels. Surface treatments are often used to improve the strength and other properties of surface and subsurface layers of hot-

working dies in order to alleviate the damages due to both thermal stress and mechanical stress, to hold back the nucleation and propagation of heat checking, and to prolong the service life of hot working dies. Other steel dies including PVD coated ledeburitic cold working steels have been invested in the past for semi-solid forming [2].

Laser glazing is a surface treatment process that forms an amorphous layers by rapid heating and quick quenching process. This amorphous structure is hard, wear-resistance, oxidation-resistance and corrosion resistance. Once the surface of the steel becomes amorphous, it becomes non-conductive, so more corrosion resistance properties are obvious [3-5]. The present work focuses to investigate the effect of processing parameters during developing an amorphous structure.

## 2 EXPERIMENTAL SET-UP

### 2.1 Experimental rig

A 1.5 kW CO<sub>2</sub> laser machining centre was used for the surface processing in this work. The pulse repetition rate could be varied by altering the frequency of the laser's master clock (4MHz). The specifications for this laser system can be seen in table 1.

Table 1: CO<sub>2</sub> laser machining centre settings

|                              |                   |
|------------------------------|-------------------|
| <b>Power (W)</b>             | 825 - 1500        |
| <b>Beam geometry</b>         | Circle            |
| <b>Focus</b>                 | Surface           |
| <b>Spot size (mm)</b>        | 0.2               |
| <b>Traverse speed (mm/s)</b> | 700 - 1200        |
| <b>Overlap (%)</b>           | 10 - 30%          |
| <b>Assist gas</b>            | Argon             |
| <b>Laser Mode</b>            | TEM <sub>00</sub> |
| <b>Operation Mode</b>        | Continuous        |

A spiral laser path processed on 10mm diameter and 100 mm long section of H13 rods was used with overlapping exposures. In order to achieve effective coverage and cooling rate in the samples a device was built that could rotate the bars while the laser spot was moved along its length. This created the required helical pattern along the entire length of the workpieces and ensured complete coverage and total

surface treatment. The diminutive exposure time required to achieve glazing indicated that rotational speeds above 1000 rpm were required. This therefore called for a reasonable powerful motor with variable speed that had a tightly integrated motor and clamp/chuck that did not deflect from the centreline.

### 2.2 Experimental procedure

The processing parameters investigated are shown in table 2. Based on previous work [4-6], the exposure times required could be estimated. These were calculated by dividing the diameter of the spot size by the point speed. The motor speed in turn could then be calculated by dividing the point speed required by the circumference of the cylinder. The irradiance was calculated by dividing the power of the laser beam by the affected area or spot size. Metallographic samples for the processed rods were prepared using Nital etchant. Vickers hardness (HV) and micro hardness (HM) measurement were made through the coating thickness.

Table 2: Laser Irradiance and exposure time settings

|    | <b>Power %</b> | <b>Irradiance (W/cm<sup>2</sup>)</b> | <b>Exposure Time (s)</b> |
|----|----------------|--------------------------------------|--------------------------|
| 1  | 100            | 4774648.3                            | 0.00029                  |
| 2  | 70             | 3342253.8                            | 0.00029                  |
| 3  | 80             | 3819718.6                            | 0.00029                  |
| 4  | 65             | 3103521.4                            | 0.00029                  |
| 5  | 60             | 2864789                              | 0.00029                  |
| 6  | 55             | 2626056.6                            | 0.00029                  |
| 7  | 70             | 3342253.8                            | 0.00025                  |
| 8  | 65             | 3103521.4                            | 0.00025                  |
| 9  | 60             | 2864789                              | 0.00025                  |
| 10 | 55             | 2626056.6                            | 0.00025                  |
| 11 | 70             | 3342253.8                            | 0.00021                  |
| 12 | 65             | 3103521.4                            | 0.00021                  |
| 13 | 60             | 2864789                              | 0.00021                  |
| 14 | 55             | 2626056.6                            | 0.00021                  |
| 15 | 70             | 3342253.8                            | 0.00017                  |
| 16 | 65             | 3103521.4                            | 0.00017                  |
| 17 | 60             | 2864789                              | 0.00017                  |
| 18 | 55             | 2626056.6                            | 0.00017                  |

### 3 RESULTS

#### 3.1 Hardness and coating thickness

The hardness and coating thickness results determined are shown in table 3. Figure 1 shows the through thickness micro-hardness stress relief plots for sample 17.

Table3: Hardness and coating thickness results.

| Sample | Substrate |      | Coating |      | Average coating thickness, micron |
|--------|-----------|------|---------|------|-----------------------------------|
|        | HV        | HM   | HV      | HM   |                                   |
| 1      | 256       | 2380 | 263     | 2430 | 50                                |
| 2      | 290       | 2666 | 607     | 4847 | 100                               |
| 3      | 270       | 2499 | 259     | 2373 | 150                               |
| 4      | 336       | 2957 | 696     | 4998 | 180                               |
| 5      | 280       | 2499 | 600     | 4765 | 160                               |
| 6      | 280       | 2499 | 665     | 4802 | 50                                |
| 7      | 275       | 2481 | 470     | 2814 | 160                               |
| 8      | 280       | 2499 | 659     | 4754 | 70                                |
| 9      | 336       | 2957 | 628     | 4958 | 150                               |
| 10     | 295       | 2695 | 600     | 4765 | 60                                |
| 11     | 240       | 2220 | 219     | 2036 | 10                                |
| 12     | 325       | 2937 | 592     | 3946 | 150                               |
| 13     | 374       | 2512 | 497     | 4191 | 50                                |
| 14     | 232       | 2134 | 316     | 2464 | 50                                |
| 15     | 298       | 2654 | 502     | 4077 | 40                                |
| 16     | 286       | 2610 | 597     | 4767 | 40                                |
| 17     | 291       | 2678 | 530     | 4357 | 40                                |
| 18     | 285       | 2609 | 754     | 5738 | 40                                |

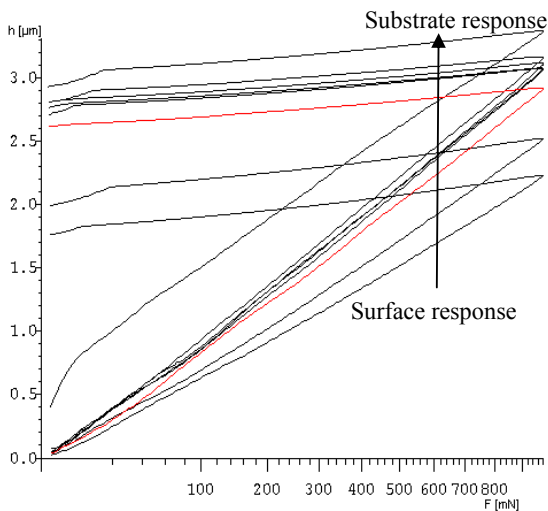


Fig. 1 Stress relief plots for a depth limited micro-hardness setting of 1 N.

#### 3.2 Metallography

Figure 2 and 3 show the through surface microstructures for six of the H13 tool steel specimens. It can be seen in these figures that samples 13, 14, and 17 showed three distinct through thickness microstructural regions. Sample 16 also showed a similar three zone effect. It is thought that a glazed region has been produced near the surface of these samples. This is the specimen skin region. The middle region has a grain growth toward the centre of the specimen, which indicates the thermal gradient was in this direction, from a hotter outer temperature to a cooler inner specimen which conducted the heat away. The final zone is a transition to the underline pearlitic substrate. Samples one and three show a ferritic type directionally solidified skin similar in microstructure to the middle zone in samples 13, 16, and 17. Sample four shows a martensitic acicular type structure when viewed at high magnification.

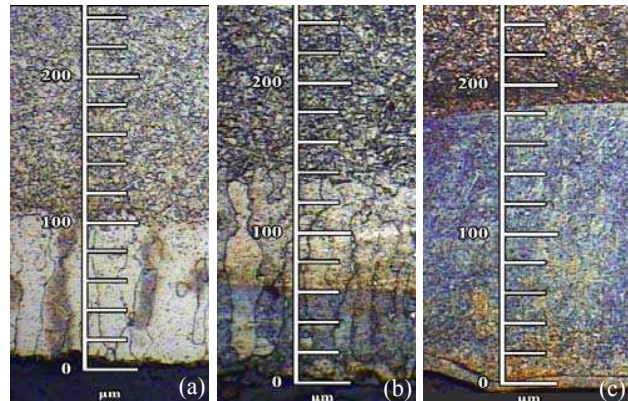


Fig. 2 Through surface micrographs of H13 tool steel laser treated specimens for (a) sample 1; (b) sample 3; and (c) sample 4.

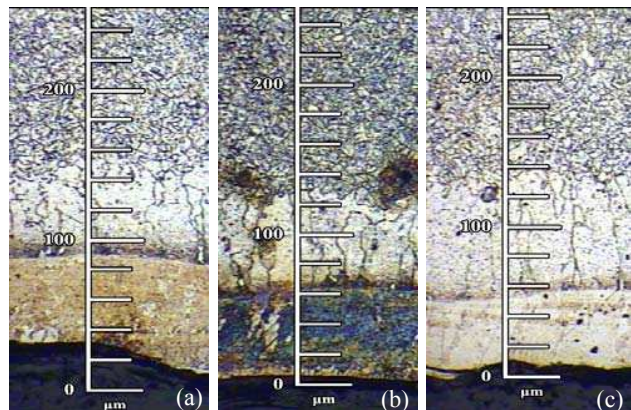


Fig. 3 Through surface micrographs of H13 tool steel laser treated specimens for (a) sample 13; (b) sample 14; and (c) sample 17.

## 4 CONCLUSIONS

Two sets of Vickers hardness readings from sample one and sample 17 are shown in figures 4 and 5 respectively. A weight of 981 mN was loaded on the indenter for these tests. The soft coating on sample one showed no improvement in surface hardness relative to the substrate, see figure 4.

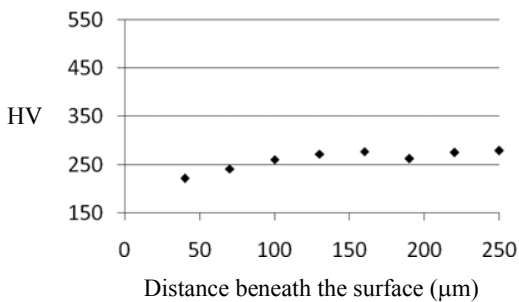


Fig. 4 Average Vickers hardness (HV) measurements taken at set distances below the surface for sample 1.

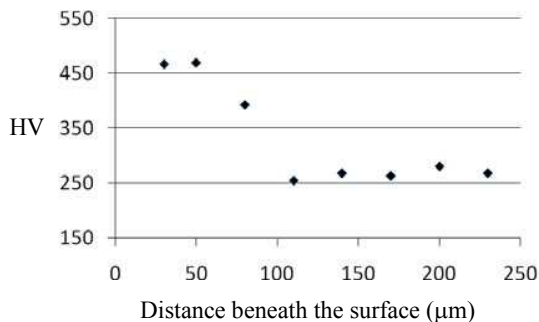


Fig. 5 Average Vickers hardness (HV) measurements taken at set distances below the surface for sample 17.

Sample 17 represented an intermediate case with noticeable improvements in surface hardness relative to the substrate recorded, see figure 5. The hardest surfaces achieved were from the processing conditions for samples 2 to 9. While microstructural changes up to 500 micrometers were noted, coating thicknesses typically of 150 micrometers were found for these samples.

The method by which the hardness is increased in the samples is seen to be dependent on rate and intensity of heat deposited. In all cases investigated here the surface was locally melted. Higher powers and lower exposure times were seen to result in

directionally solidified ferritic skin layers and relatively soft surfaces, as for sample one. Lower powers and exposure times results in a tri-zoned microstructure with intermediate surface hardness, as for sample 17. Highest hardness was achieved with the intermediate irradiances and exposure times as for sample 4, where a surface hardness of about 700 HV was achieved. Surface glazing may have occurred in these samples. The large increases in hardness values observed (up to four times that of the substrate) indicate great potential for use in semi-solid steel processing. Another advantage of glazing the surface is the potential ability from this process to tailor a thermal shock barrier for the underlying die surface [7].

## ACKNOWLEDGEMENTS

The authors would like to acknowledge the technical support from Martin Johnson and Michael May in performing this study. The authors would also like to acknowledge the support from the School of Mechanical and Manufacturing Engineering at Dublin City University and the COST 541 Project.

## REFERENCES

1. R.A. Higgins, *Engineering metallurgy: applied physical metallurgy*, 1983, ISBN 0-340-28524-9.
2. Knauf, F., Hirt, G., Immich, P., Bobzin, K., Influence of tool geometry, tool coating and process parameters in Thixoextrusion of steel, *Proceedings of the Int. Conf ESAFORM 10, Zaragoza (2007)*
3. Matthews, D., Ocelik, V., De Hosson, J., Tribological and mechanical properties of high power laser surface-treated metallic glasses, *Materials Science and Engineering: A*, In Press, Corrected Proof.
4. Jiang, W., Molian, W., Molian, P., Nanocrystalline TiC powder alloying and glazing of H13 steel using a CO<sub>2</sub> laser for improved life of die-casting dies, *Surface and Coatings Technology*, 2001, Vol.135, pp.139-149.
5. Yang, Y., Song, Y., Wu, W., Wang, M., Multi-pass overlapping laser glazing of FeCrPC and CoNiSiB alloys. *Thin Solid Films*, 1998, 323, 199-202.
6. Ready, J., *LIA Handbook of Laser Material Processing*, Magnolia Publishing, Inc., Orlando, 2001.
7. Wang, K., Fujita, T., Chen, W., Nieh, T., Okada, H., Koyama, K., Zhang, W., Inoue, A., Electrical conductivity of a bulk metallic glass composite, *Applied Physics Letters*, 91, 154101, 2007.